Microsystems for the Capture of Low-Abundance Cells

Udara Dharmasiri,[1,3] Małgorzata A. Witek,[1,3] Andre A. Adams,[1,4] and Steven A. Soper[1,2,3]

Departments of [1]Chemistry and [2]Mechanical Engineering and [3]The Center for Biomodular Multi-Scale Systems, Louisiana State University, Baton Rouge, Louisiana 70803; email: udharm1@tigers.lsu.edu, mwitek@lsu.edu, aadadams@alumni.lsu.edu, chsope@lsu.edu

[4]Center for Bio/Molecular Science and Engineering, Naval Research Laboratory, Washington, DC 20375

Annu. Rev. Anal. Chem. 2010. 3:409–31

First published online as a Review in Advance on April 1, 2010

The *Annual Review of Analytical Chemistry* is online at anchem.annualreviews.org

This article's doi: 10.1146/annurev.anchem.111808.073610

1936-1327/10/0719-0409$20.00

Key Words

cell capture and enumeration, circulating tumor cells, size-based selection, immunoaffinity capture, fluorescence-activated sorters, dielectrophoretic separation

Abstract

Efficient selection and enumeration of low-abundance biological cells are highly important in a variety of applications. For example, the clinical utility of circulating tumor cells (CTCs) in peripheral blood is recognized as a viable biomarker for the management of various cancers, in which the clinically relevant number of CTCs per 7.5 ml of blood is two to five. Although there are several methods for isolating rare cells from a variety of heterogeneous samples, such as immunomagnetic-assisted cell sorting and fluorescence-activated cell sorting, they are fraught with challenges. Microsystem-based technologies are providing new opportunities for selecting and isolating rare cells from complex, heterogeneous samples. Such approaches involve reductions in target-cell loss, process automation, and minimization of contamination issues. In this review, we introduce different application areas requiring rare cell analysis, conventional techniques for their selection, and finally microsystem approaches for low-abundance-cell isolation and enumeration.

1. LOW-ABUNDANCE CELLS

Low-abundance cells: cells present at concentrations less than 1,000 cells ml^{-1} of fluid sample

Circulating tumor cells (CTCs): cells released from a primary tumor into circulation and carried to a secondary site, where they can spawn metastatic disease

What distinguishes a low-abundance cell from one that is not, and what applications require the ability to analyze low-abundance cells? On the basis of the data presented in **Table 1**, we consider any sample containing less than 1,000 target cells ml^{-1} to contain low-abundance cells. Typical examples of low-abundance cells are circulating tumor cells (CTCs), circulating fetal cells, and stem cells. The abundance of these cells, as well as others, is highly variable and depends upon factors such as the age of the sample, the stage of the disease, and the cellularity, which is defined as the state of a tissue or cell with regard to the degree, quality, or condition of cells present (1). However, environmental samples containing biopathogens are categorized on the basis of the effective infectious dose level that can lead to the outbreak of disease (**Table 1**).

The ability to select and enumerate low-abundance cells and their subsequent analyses have many important applications (**Table 1**), such as cancer research (2), forensic science, homeland

Table 1 Low-abundance cell types (<1000 targets ml^{-1}) and methods for their selection[a]

Rare cell type	Resident material	Cell abundance (cells ml^{-1})	Selection method	Reference(s)
CTCs: lung, breast, prostate, pancreas, colon, cervix, bladder	Peripheral and cord blood, bone marrow, lymph, thymus, urine	0.3–100	IMACS, FACS, affinity columns	6, 9, 88
Fetal: trophoblasts, lymphocytes, nucleated RBCs	Maternal and cord blood	1–15	IMACS, FACS, charge flow separation, DGC	65
Stem: progenitor cells	Peripheral and cord blood, bone marrow	10–400	IMACS, FACS, affinity columns, DGC	89–91
Somatic: Sperm	Vaginal swab	380	Differential extraction, FACS	92
Infected: HIV-infected T cells, *Streptococcus* spp.–infected lymphocytes	Peripheral blood, lymph	1–300	IMACS, FACS, affinity columns, ELISA	78, 93, 94
Bacteria: *Enterococcus hirae*, *E. gallinarum*, *Streptococcus pneumoniae*, *Escherichia coli* O157:H7, *Vibrio cholerae*	Waste, river, and drinking water	0.01–1	Bacterial cultures, ELISA, PCR/RT-PCR	84, 95[b]
Virus: Adenoviruses, enteroviruses, hepatitis A and E	Waste, river, and drinking water	0.01–1	Viral cultures, affinity columns, RT-PCR, ELISA	See footnote b
Dengue	Peripheral blood, lymph	1–1000	Viral cultures, affinity columns, RT-PCR, ELISA	54, 95, 96
Swine flu	Peripheral blood, lymph	1–610	Viral cultures, affinity columns, RT-PCR, ELISA	54, 95, 96
Bovine diarrhea	Peripheral blood, lymph	1–10	Viral cultures, affinity columns, RT-PCR, ELISA	54, 95, 96
Protozoa/helminthes: *Cryptosporidium parvum*, *Entamoeba histolytica*, *Naegleria fowleri*, *Dracunculus medinensis*	Waste, river, and drinking water	0.01–1	Fluorescent antibody procedure, filtration, PCR/RT-PCR, ELISA	See footnote b

[a]Abbreviations: CTCs, circulating tumor cells; DGC, density-gradient centrifugation; ELISA, enzyme-linked immunosorbent assay; FACS, fluorescence-activated cell sorting; HIV, human immunodeficiency virus; IMACS, immunomagnetic-assisted cell sorting; RBCs, red blood cells; RT-PCR, reverse-transcription polymerase chain reaction.

[b]See **http://www.who.int/water_sanitation_health/gdwqrevision/watpathogens.pdf**.

security, space exploration, environmental analysis (3), isolation and characterization of intact fetal cells in maternal blood for noninvasive prenatal diagnosis (4), use of stem cells for cell-based therapies (5), detection of CTCs in blood for differential diagnosis and prognosis (6–11), and detection of T lymphocytes for determining the progression rate of human immunodeficiency virus infections (12, 13) or autoimmune disease (14). Another fast-growing area requiring low-abundance cell analysis is the isolation and detection of pathogens and protozoan parasites such as *Escherichia coli* O157:H7, swine influenza virus, and *Cryptosporidium* in various food and water samples (15–17).

The challenge in any analytical strategy for low-abundance cells begins with the selection of the target cells from a heterogeneous population in which the target is a minority. For example, in the case of CTCs, in 1 ml of whole blood there are more than 10^9 red blood cells (RBCs) and typically one to five CTCs, requiring an enrichment factor less than 10^9. For the isolation of low-abundance cells, four important metrics must be considered: (*a*) throughput, the number of cell-identification or -sorting steps per unit time; (*b*) recovery, an indicator of the fraction of target cells collected from the input sample; (*c*) purity, which depends on the number of so-called interfering cells excluded from the final analysis; and (*d*) viability, that is, whether the isolated cells retain their biological function after the selection process (18, 19). Additionally, highly efficient quantification of the number of enriched low-abundance cells must be provided in most cases (20).

RBCs: red blood cells; erythrocytes

Throughput: the number of cell-identification or -sorting steps per unit time

Recovery: refers to the fraction of target cells collected from the input sample

Purity: refers to the fraction of so-called interfering cells excluded from the analysis

Viability: characterizes isolated cells that retain their biological function after the sorting process

IMACS: immunomagnetic-assisted cell sorting

FACS: fluorescence-activated cell sorting

RT-PCR: reverse-transcription polymerase chain reaction

2. METHODS FOR LOW-ABUNDANCE-CELL SELECTION

Two basic formats can be used for selecting low-abundance cells from mixed populations: macro- and microscale formats. Macroscale formats provide high throughput for selecting low-abundance cells due to their ability to process large input volumes quickly, whereas microscale formats typically lack that ability (see **Figure 1**) (21). High-throughput processing is required due to the necessity for sampling large input volumes to generate a high statistical confidence for successfully securing the target cells from the processed sample. Throughput is directly proportional to (*a*) the cross-sectional area of the conduit through which the sample is delivered and (*b*) the rate of sample delivery. The input sample volume required for the assay is determined by the frequency of rare cell appearance. For example, at 5 cells ml^{-1}, a sampling volume of 1 μl would produce a probability of only 0.5% of finding the target cells in that volume. Because low-abundance cells appear at frequencies less than 1,000 cells ml^{-1}, high-volume sampling (≥1 ml) is required to increase the probability of isolating these rare events. If cross-sectional dimensions of 35 μm × 35 μm were employed for a fluidic conduit to exhaustively search for rare cells, and if the transport rate through the conduit were 10 mm s^{-1} with a required input volume of 1.0 ml, the sampling time would be approximately 278 h. For a single rectangular conduit with dimensions of 150 μm × 35 μm under conditions similar to those given above, the sampling time would be reduced to ∼5.6 h. If the 150 μm × 35 μm conduits were highly parallelized through the incorporation of 51 conduits, the processing time would drop to 0.12 h (**Figure 1**).

2.1. Macroscale Techniques for Selecting Low-Abundance Cells

Commonly used macroscale formats for enriching low-abundance cells include (*a*) magnetic capture that employs micrometer-sized ferromagnetic beads coated with molecular recognition elements, typically referred to as immunomagnetic-assisted cell sorting (IMACS) (22–24); (*b*) size-based separations that use nuclear-tracked membranes (25, 26); (*c*) fluorescence-activated cell sorting (FACS) (27, 28); and (*d*) reverse-transcription polymerase chain reaction (RT-PCR) of

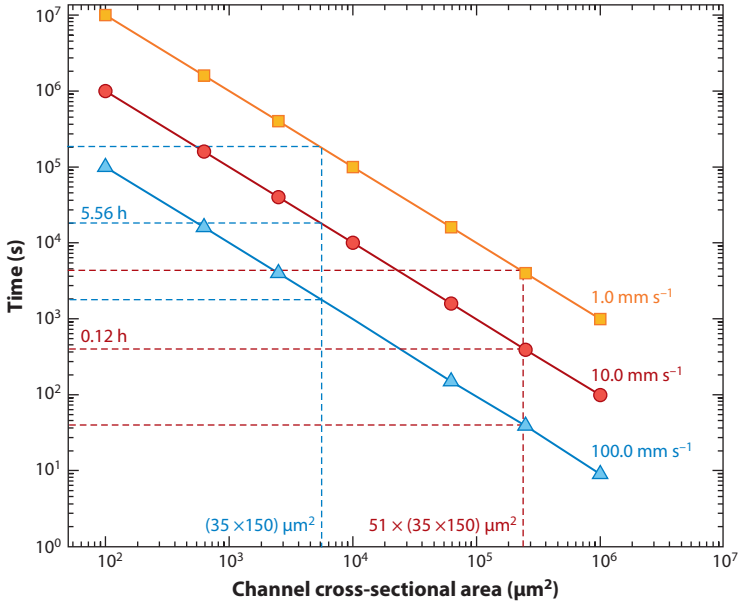

Figure 1

Sample-processing time as a function of the fluidic conduit cross-sectional area at three different linear velocities: 1, 10, and 100 mm s^{-1}. Reproduced with permission from Reference 21.

messenger RNAs (mRNAs), which are used as surrogates for cell identification (29). In the following sections, we briefly discuss these macroscale processing techniques.

2.1.1. Immunomagnetic-assisted cell sorting. CellSearch™ is a commercially available IMACS system for selecting CTCs from peripheral blood (30). It employs anti-epithelial cell adhesion molecule (anti-EpCAM) antibodies for selecting CTCs from 7.5 ml of peripheral blood. In one study, the sample was incubated with ferromagnetic particles coated with anti-EpCAM antibodies, and the immunomagnetically labeled cells were isolated by an external magnetic field (**Figure 2*a*–*c***) (31). Following magnetic isolation, the processed sample was incubated with leukocyte-specific CD45 antibodies labeled with Alexa Fluor 555®, nuclear-specific 4′,6-diamidino-2-phenylindole (DAPI), and CTC-specific cytokeratin antibodies conjugated to a fluorescein derivative. CTCs were identified as positive for cytokeratins and DAPI but negative for CD45. A rigorous evaluation of the performance metrics of the CellSearch system indicated that the CTC recovery was ~85% (6).

EpCAM: epithelial cell adhesion molecule

Antibodies: gamma globulin proteins found in the body fluids of vertebrates; used by the immune system to recognize and neutralize foreign objects

2.1.2. Size-based selection. Tracked polycarbonate membranes with varying pore sizes (8–14 μm) can be employed to filter large sample volumes (9–18 ml) containing low-abundance cells. Zabaglo et al. (32) selected CTCs directly from whole blood through the use of tracked membranes. The samples were diluted at a 1:1 volume/volume (v/v) ratio with phosphate-buffered saline, which contained an anticoagulant. After the initial filtration, the isolated cells were incubated with anti–pan cytokeratin antibodies labeled with fluorescein-isothiocyanate directed against cytokeratins 5, 6, 8, 17 and 19. Following a wash to remove the unbound anti-cytokeratin antibodies, nuclei-specific propidium iodide was added, and the cells retained by the tracked membrane were analyzed with a combination of laser scanning cytometry and microscopy. Only positive cells

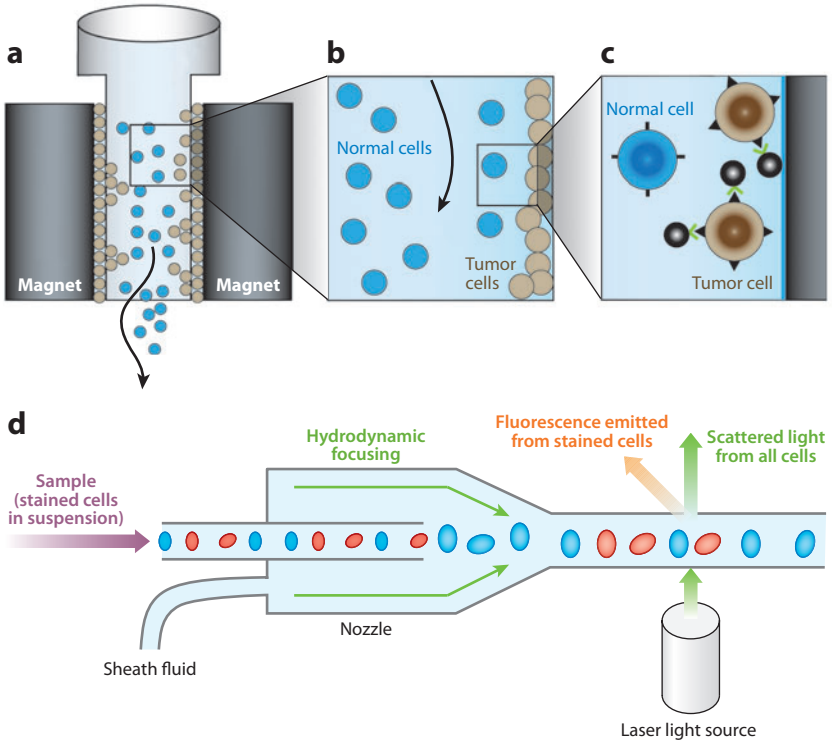

Figure 2

(*a–c*) Schematic of the immunomagnetic-assisted cell-sorting process. Blue and tan circles represent normal and circulating tumor cells, respectively. Reproduced with permission from Reference 31. (*d*) Schematic of a fluorescence-activated cell-sorting instrument. Adapted from **http://www.abcam.com/technical**.

with the appropriate nuclear-to-cytoplasmic ratio were counted as CTC events. These membranes isolated nearly 85%–100% of the CTCs from whole blood, but the captured cells were of low purity due to significant retention of white blood cells (WBCs).

2.1.3. Fluorescence-activated cell sorting. FACS can be used to select low-abundance cells from mixed populations by monitoring the presence of antigenic species indigenous only to the target cells (see **http://www.abcam.com/technical**). FACS samples individual cells in a high-throughput fashion (~50,000 cells s^{-1}) by monitoring the fluorescence signature elicited by each cell type (**Figure 2*d***). For example, FACS has been used to detect and enumerate an immortalized breast cancer cell line (BT-20 cells) that was seeded into peripheral blood mononucleated cells (PBMCs) at frequencies of 10^{-5}, 10^{-6}, and 10^{-7} (33). The flow cytometer employed three excitation wavelengths, 325, 488, and 633 nm, allowing for discrimination between the PBMCs and the BT-20 cells. A panel of fluorescently labeled antibodies allowed the BT-20 cells to produce distinct colors for their identification from the PBMCs. BT-20 cells were also characterized by a cocktail containing three anti-cytokeratin antibodies, each tagged with a different-colored dye. Through the use of a color-discrimination algorithm, BT-20 cells were detected with a 20% recovery for frequencies at 10^{-5} and 10^{-6}. The challenges associated with this assay format were the extensive amount of time required for the immunofluorescent staining (~20 h), the need to remove the RBCs from the blood sample prior to processing, and the extensive equipment required for the

WBCs: white blood cells; leukocytes

measurements. The recovery was low due to the loss of target cells during removal of the RBC fraction and the extensive staining and processing steps required. For this approach to reliably assess rare CTCs at frequencies of 10^{-7} in the presence of PBMCs, ~200 ml of blood would be needed.

DGC: density-gradient centrifugation

2.1.4. Molecular methods. Another approach employed for the analysis of low-abundance cells in clinical or environmental samples is RT-PCR, in which mRNAs are used as markers to report on the presence of specific low-abundance cells. For example, reports have documented RT-PCR's ability to detect low-abundance cells in 10^6 PBMCs via an appropriate marker panel (34). Gene expression–based assays have high sensitivity but can generate poor selectivity, which can lead to false-positive results. Also, as with many low-abundance cell–based assays for whole blood, the RBC fraction must be removed with, for example, Ficoll-Hypaque density-gradient centrifugation (DGC), which can reduce cell recovery. Notably, these assays are prone to high interlaboratory variability (35).

Microarrays can also be used to isolate rare cells via so-called cluster of differentiation (CD) antigens that are unique to the target cell type (36). The arrays contain several surface-immobilized antibodies directed toward target CD-antigenic species, which are used to spatially isolate the cells. These methods are limited by slow mass transport, but they can provide highly multiplexed analyses. Unfortunately, the array elements are not individually addressable, making collection of the isolated cells difficult due to the single-chamber format of the arrays. Belov et al. (36) presented an array technique based on CD for the treatment of leukemia. The CD antigens were used to phenotype leukocytes on the basis of characteristic abnormal patterns of antigen expression. Microarray technology has also been used to screen human immunodeficiency virus–positive blood against normal blood (37).

2.2. Challenges Associated with Macroscale Methods for Low-Abundance-Cell Selection

Enrichment of target cells via macroscale systems typically employs either positive selection (for example, IMACS or FACS) or negative selection. Negative selection gives low purity (0.01%–0.1%) due to insufficient removal of interfering cells (38). When the sample matrix is whole blood, negative selection performed on the basis of size is often marred by interferences resulting from leukocytes, due to the similarity in size between these cells and the CTCs, for example (39, 40). Attempts to further preconcentrate targets and remove WBCs introduce a significant risk of target loss. For example, monocytes were found to interfere with the selection of comparably sized stem cells (41).

The challenges associated with positive selection using IMACS or FACS assays are the extensive amount of time required for the immunofluorescent staining (~20 h) and, in many cases, the need to remove the RBCs from a blood sample prior to processing. Furthermore, semiautomated processes requiring operator intervention and the variability in reagent and laboratory protocols lead to poor interlaboratory standardization and data collection, assessment, and management (42). Additionally, downstream processing of the collected rare cells requires samples with high purity that are in a viable form (i.e., following cell culturing). For example, the magnetic field used for IMACS may produce perturbations on stem cell differentiation (43). Finally, in the case of positive selection, the recovery can depend upon the expression level of the antigenic membrane protein used for their selection (9).

Many macroscale techniques also rely on DGC preselection. Differences in density between cell types can be small, and individual cell types can be heterogeneous in size and density (44).

Consequently, particular cell types can distribute throughout a density-gradient medium, rather than precisely segregate at a discrete area; this results in reduced recovery of the desired cells and/or contamination with undesired cell types (45). Procedures such as DGC that enrich for low-abundance blood cell types, such as hematopoietic progenitor cells, can lead to significant loss or reduced yields due to poor segregation with potential interfering cells. For example, conventional density-gradient methods to isolate progenitor cells (e.g., $CD34^+$ hematopoietic stem cells) from umbilical cord blood results in significant loss of the desired stem cells (46).

Aptamers: oligonucleotides, either single-stranded RNAs or DNAs, that have the ability to recognize certain targets such as proteins

3. MICROSYSTEMS FOR LOW-ABUNDANCE-CELL SELECTION

Microsystem technologies allow the dissemination of new sample-processing capabilities to a broader user community due to their potentially smaller footprint, lower power consumption, reduced reagent requirements, and process automation, as compared with their benchtop counterparts. Additionally, improved performance is fundamental to high-sensitivity cellular analysis technologies (47, 48). In particular, microsystem platforms enable one to handle small numbers of cells without loss. Such a task is difficult to achieve with instruments such as conventional flow cytometers, which typically require a starting population of more than 100,000 cells (49). Furthermore, low-abundance cell–selection mechanisms such as affinity, physical characteristics, dielectrophoresis (DEP), and magnetic interactions can be integrated into a microsystem, along with downstream molecular processing of the intracellular contents of the selected cells, to provide important clinical or environmental information. The challenge for imposing low-abundance cell–selection assays to microsystems is sampling; to generate a high statistical probability of selecting the low-abundance cells, large input volumes (>1 ml) must be processed, and most microsystems cannot handle large-volume inputs in reasonable times (i.e., they have poor throughput; see **Figure 1**). Therefore, novel design approaches must be implemented to accommodate the necessary sampling volume. In the following sections, we review microfluidic-based systems for selecting low-abundance cells.

3.1. Low-Abundance-Cell Selection via Immunoaffinity Interactions

Affinity-based selection of low-abundance cells is often employed in microsystems. This approach exploits the specific but noncovalent interactions between a ligand, such as an antibody, aptamer, or peptide, and a target-specific receptor, such as a membrane protein (50). Affinity-based cell selection via microsystems can be carried out by either positive or negative selection. Negative selection requires the complete removal of the nontarget cells with minimal target-cell capture and is an attractive approach when the specific markers for target cells are not fully known. In contrast, positive selection involves directly capturing the target cell through the use of a membrane protein(s) unique to that cell type (9).

In most cases, cell selection involves a solid phase in which (*a*) the recognition element(s) is covalently tethered to the surface of a fluidic conduit and (*b*) the sample containing the low-abundance cells is moved through this conduit to invoke the selection process. The operational criteria mentioned in Section 1 are important to this phase, as are (*a*) nonspecific interactions, (*b*) target cell–recognition element adhesion strength, (*c*) conduit architecture, (*d*) recognition element immobilization chemistry, and (*e*) ligand surface density.

As noted in Section 1, throughput—namely, the number of cell-identification or -sorting steps per unit time—is a critical metric to optimize. One can improve throughput by increasing the transport rate of sample through the selection conduit. However, cell recovery can degrade at certain transport rates, indicating that there is an optimal flow rate at which the system can

be operated. The analytical model used to explain this observation is based on cell adhesion between a surface-tethered antibody and a moving antigen (51). This model describes a two-state process. The first state accounts for transport of the solution-cell antigen to the surface-bound antibody, which describes the encounter rate (k_o). The second state gives the probability (P) that an association event will occur during the time the antigen is in close proximity to the tethered antibody. The encounter rate, k_o, increases linearly with flow velocity, whereas P decreases. These states can be used to calculate the rate of capture per antigen-antibody pair (k_f, s^{-1}) via the following equation (51):

$$k_f = k_o P. \tag{1}$$

P can be estimated from Equation 2,

$$P = \Lambda\delta/(1 + \Lambda\delta), \tag{2}$$

where δ is the dimensionless Damköhler number (calculated from $a^2 k_{in}/D$; k_{in} is the intrinsic antigen-antibody reaction rate; a is the encounter radius) and Λ is the dimensionless encounter time [calculated from $\tau/(a^2/D)$; $\tau = 8a/(3U\pi)$; U is the cell-translational velocity; D is the cell-diffusion coefficient (20, 51)]. Equation 1 indicates that the recovery increases with translational velocity due to increases in k_o but that, beyond an optimal velocity, the recovery degrades due to insufficient reaction time (i.e., lower P).

Critical to affinity-based cell selection that uses surface-immobilized recognition elements and flow processing is the adhesion force (F_A) between the cell and the antibody-decorated surface, which must be greater than the shear force (F_S) generated by the solution flow to prevent target-cell loss. F_A can be determined from the bond strength between a single antigen-antibody complex (f_c), the cell-contact area with the recognition surface (A_c), and the number of receptors poised on the surface within the contact area of the cell (C_s). F_A is calculated from (20)

$$F_A = f_c \times A_c \times C_s. \tag{3}$$

If the cell is assumed to be a nondeformable object once it adheres to the capture surface, the contact area can be calculated from Equation 4 (52),

$$A_c = \pi\{r_p \sin[\cos^{-1}(r_p - h' + h)/r_p]\}^2, \tag{4}$$

where r_p is the cell radius and h and h' represent the characteristic cell-separation distances from the surface upon binding. When the F_S generated by the flow is equal to or greater than F_A, the cell can be removed from the surface. The velocity-dependent F_S can be determined from Stokes's law (53),

$$F_S = 6\pi\eta r_p v_c, \tag{5}$$

where r_p is the cell radius, η is the solution viscosity, and v_c is the critical linear velocity that can induce cell detachment.

Nagrath et al. (9) developed a microsystem for selecting CTCs directly from peripheral blood. The CTCs originated from solid lung, colorectal, breast, prostate, brain, and neck tumors and were selected through use of anti-EpCAM monoclonal antibodies tethered to the walls of a microfluidic channel and posts. The device contained 78,000 microposts that were 100 μm tall and 100 μm wide with a total surface area of 970 mm^2 (**Figure 3**). Anti-EpCAM monoclonal antibodies provided the specificity for CTC recovery from unfractionated blood because EpCAM is specifically overexpressed by adenocarcinomas (9, 20). The essential parameters that determined recovery by the CTC chip were flow velocity, shear force, and cellular EpCAM expression level, as noted in Equations 1–5. At a flow rate of 1 ml h^{-1}, 65% of the CTCs were recovered, and 98% of the cells remained viable. As the processing flow rate was increased to 3 ml h^{-1}, the

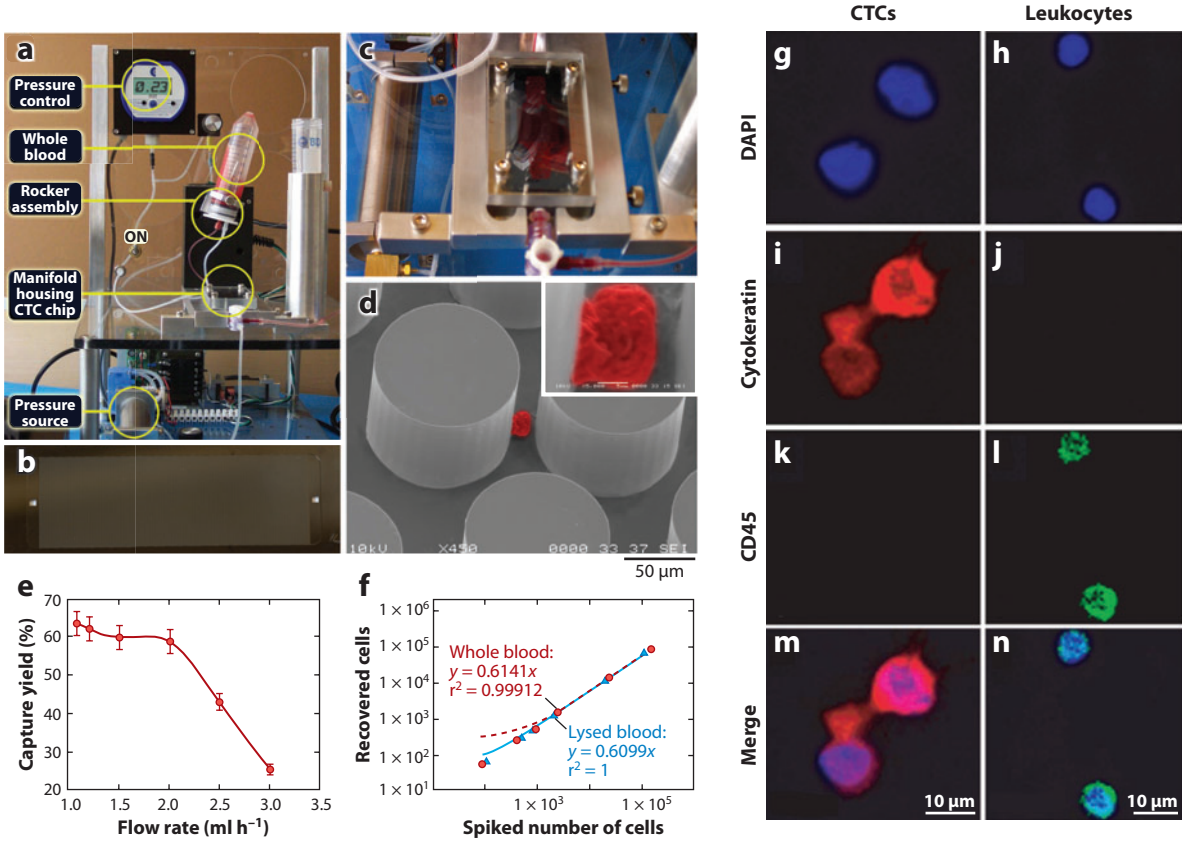

Figure 3

Isolation of circulating tumor cells (CTCs) from whole blood, performed with a microfluidic device (CTC chip) fabricated in silicon via reactive ion etching. (*a*) The workstation setup for CTC isolation from whole blood. (*b*) The CTC chip with microposts etched into the silicon. (*c*) Micrograph of whole blood flowing through the CTC chip. (*d*) An image of a captured NCI-H1650 lung cancer cell spiked into blood (pseudo-colored red). The inset shows a high-magnification view of the captured cell. (*e*) CTC recovery as a function of flow rate. (*f*) Regression analysis of capture efficiency for various target-cell concentrations in whole-blood samples versus lysed-blood samples. (*g–n*) High-magnification images of captured CTCs and hematologic cells stained with 4′,6-diamidino-2-phenylindole (DAPI), cytokeratin, and CD45. Merged images identify CTCs in panels *g*, *i*, *k*, and *m* and hematologic cells in panels *h*, *j*, *l*, and *n*. Reproduced with permission from Reference 9.

recovery was reduced to 25%, as shown in **Figure 3*e***. Enrichments from whole blood provided ~50% purity, and as a result the CTCs had to be differentiated from the major impurity, leukocytes, through use of fluorescently labeled cytokeratin and CD45 antibodies (**Figure 3*g–n***). The same CTC chip was also used to select low-abundance lung cancer cells from whole blood (53). Extensive clinical studies have been successfully completed with the use of this CTC chip. For example, with this chip CTCs were isolated in 100% of patients with early-stage prostate cancer. Furthermore, the potential utility of this CTC chip in monitoring response to anticancer therapy was also investigated. In a small cohort of patients with metastatic cancer who were undergoing systemic treatment, temporal changes in CTC numbers correlated well with the clinical course of the disease (9, 53).

Adams et al. (20) introduced a microchip-based high-throughput microsampling unit (HTMSU) capable of selecting very low abundance CTCs from whole blood in a single step.

The HTMSU was fabricated from poly(methylmethacrylate) (PMMA) via microreplication and consisted of 51 ultrahigh–aspect ratio, parallel, curvilinear channels and a Pt-conductivity sensor to allow for cell enumeration (**Figure 4**). The capture channels were functionalized, via a carboxylate scaffold, with anti-EpCAM monoclonal antibodies. The authors found that the CTC-capture efficiency varied with channel width; the highest recovery (97%) was obtained for channels that had similar widths (35 μm) to the CTC dimensions (15–30 μm) (**Figure 4*f***). The device was capable of high-throughput operation at an optimal linear fluid velocity of 2 mm s^{-1} in each channel (51 parallel channels), allowing 1-ml samples to be exhaustively interrogated in ∼37 min. The captured CTCs were subsequently removed from the capture surface via trypsin and were quantitatively counted one at a time via conductivity detection.

Microsystems have also been applied to immunoassay-based recognition for pathogen detection. Static forward light scattering was investigated for the analysis of bovine viral diarrhea virus in a complex matrix mimicking a body fluid (54). The assay was based on the use of microparticles coated with antibodies directed against bovine viral diarrhea virus, and the reaction was monitored in a Y-shaped poly(dimethylsiloxane) (PDMS) fluidic device with optical fibers oriented at a 45° angle to measure light scatter from single virus cells. Bovine viral diarrhea virus concentrations of 10 $TCID_{50}$ ml^{-1} (where $TCID_{50}$ stands for 50% tissue-culture infectious dose) were detected with this microfluidic chip.

Application of antigen/antibody-recognition strategies for low-abundance-cell selection is, in some cases, limited by the availability of antibodies directed against membrane proteins uniquely found on the target rare cells (55). Additionally, most positive-selection tools require surface immobilization of the antibody, which can result in reduced recovery or adhesion strength between the cell and the surface-tethered antibody due to the stochastic nature of the immobilization chemistry. Antibodies may also show variation in antigen binding, exhibit instability when bound to solid surfaces, and have limited binding sites (29). Finally, environmental factors may affect antibody-antigen interactions (56, 57). Therefore, alternatives to antibodies for low-abundance-cell selection have been investigated.

Aptamers, single-stranded nucleic acid oligomers, possess highly specific recognition affinities to molecular targets through interactions other than classical Watson-Crick base pairing (58). Compared with antibodies, aptamers have lower molecular weights, remain stable during long-term storage, sustain reversible denaturation, have low toxicity, and can be produced against targets via highly automated technologies [e.g., SELEX (systematic evolution of ligands by exponential enrichment)] (59). Additionally, their immobilization chemistry is highly oriented: End-point attachment occurs exclusively through the 5′ or 3′ end of the aptamer, which bears a functional group. These advantages make aptamers highly desirable as potential molecular recognition elements for low-abundance-cell selection (60).

Aptamers have been employed in a microsystem for the capture of prostate cancer cells that used a LNCaP cell line as a model. This cell line overexpresses a prostate-specific membrane antigen (PSMA) that was used as a marker for the selection of these cells (61). Nuclease-stabilized and in vitro–generated PSMA aptamers were immobilized onto ultraviolet-modified PMMA capture channels (**Figure 4*a–d***). The authors used carbodiimide-coupling chemistry and the appropriate linker structure to enhance the accessibility of the surface-bound aptamer to the solution-borne cells (**Figure 5*a***). Following selection and isolation, the captured cells were released from the capture surface via enzymatic digestion of the extracellular domain of PSMA for subsequent conductivity enumeration. CTCs possess unique electrical properties that arise from their characteristic chemical composition (compared with those of erythrocytes and leukocytes), which provides efficient and selective conductivity readout (62). For example, the overexpression of membrane glycoproteins—such as PSMA and EpCAM, which are associated with many tumor

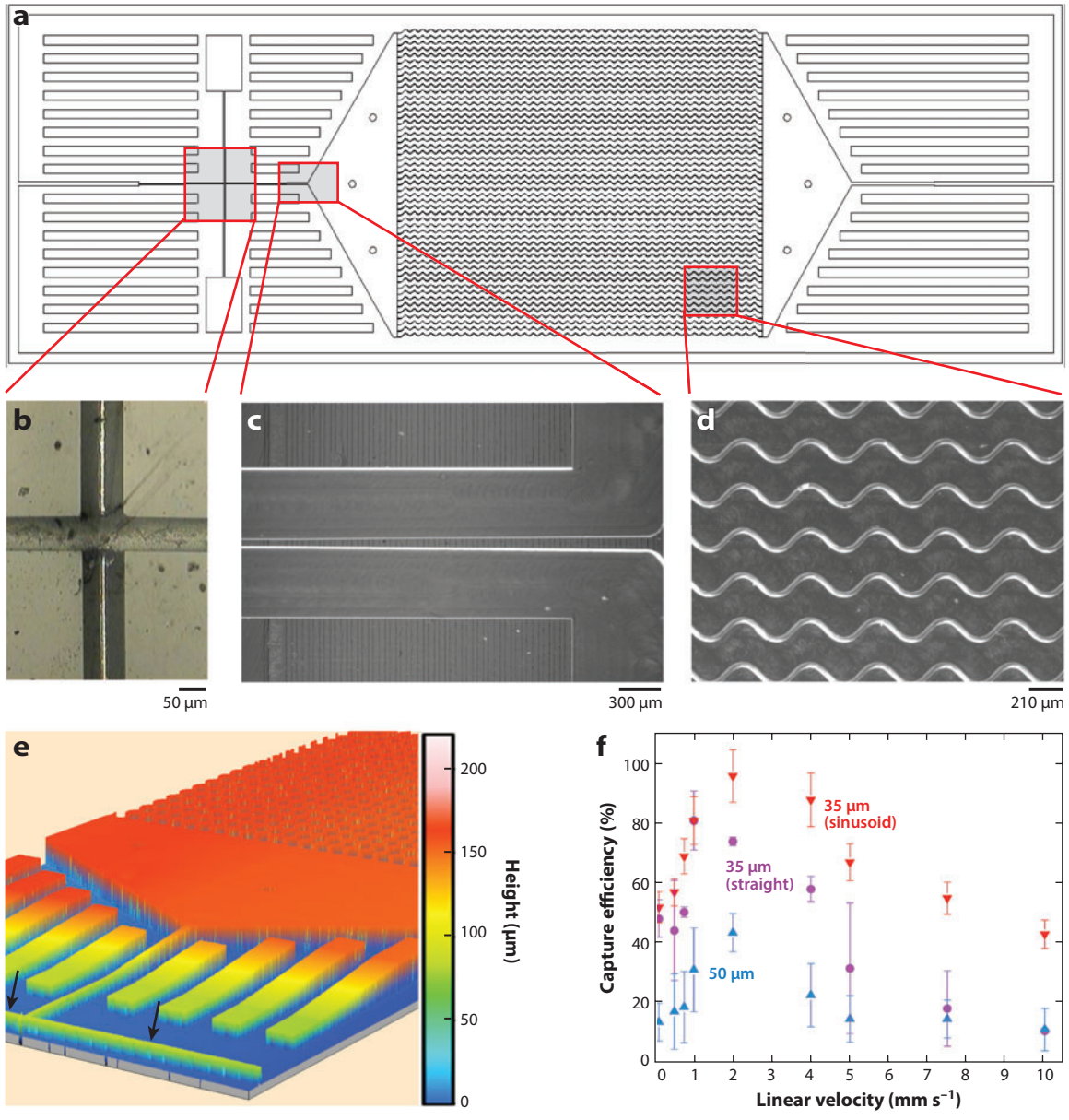

Figure 4

Schematic of a microchip-based high-throughput microsampling unit (HTMSU) fabricated in poly(methylmethacrylate) via microreplication for selection of circulating tumor cells (CTCs). (*a*) An AutoCAD® diagram of the sinusoidally shaped capture channels with bright-field optical micrographs showing (*b*) the integrated conductivity sensor consisting of cylindrical Pt electrodes with a 75-µm diameter and a 50-µm gap; (*c*) the single port exit, where the HTMSU's width tapers from 100 µm to 50 µm and the depth tapers from 150 µm to 80 µm over a 2.5-mm region that ends 2.5 mm from the Pt electrodes; (*d*) the sinusoidal cell-capture channels (5× magnification); (*e*) three-dimensional projection of the topology of the HTMSU obtained at 2.5-µm resolution via noncontact optical profilometry (*arrows*, Pt electrode conduits); and (*f*) the capture efficiency of CTCs in spiked whole-blood samples as a function of the cells' translational velocity. The microchannels were 35 µm wide (*red down triangles*, sinusoid; *purple circles*, straight) and 50 µm wide (*blue up triangles*). Reproduced with permission from Reference 20.

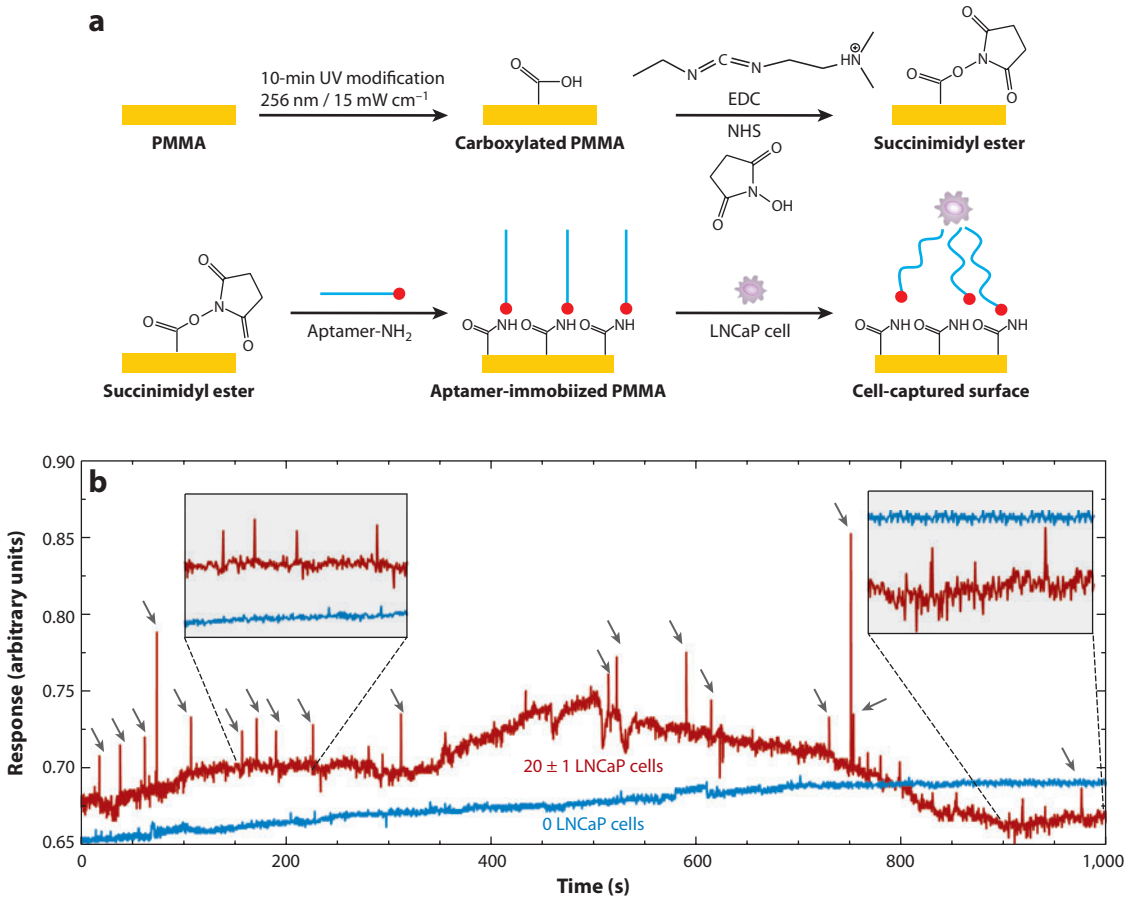

Figure 5

(*a*) Chemical steps for the immobilization of aptamers to the surfaces of a poly(methylmethacrylate) (PMMA)-based high-throughput microsampling unit (HTMSU) used for the positive selection of LNCaP cells. (*b*) Conductometric responses generated for 1.0 ml of whole blood seeded with 20 ± 1 LNCaP cells (*red*) and 0 LNCaP cells (*blue*), at a linear flow velocity of 2.5 mm s^{-1}, processed with an HTMSU. The arrows designate peaks that were identified as LNCaP cells on the basis of a signal-to-noise threshold of 3. Abbreviations: EDC, 1-ethyl,-3-(3-dimethylaminopropyl)carbodiimide; NHS, *N*-hydroxysuccinimide. Reproduced with permission from Reference 61.

or cancer cells—results in an increase in the number of negatively charged sialic acid molecules that cap the extracellular domains of these integral membrane proteins (52). As shown in **Figure 5*b***, only positive signals were designated as LNCaP cells due to their electrical properties. The system required no sample pretreatment and provided high throughput (processing time for 1 ml was 29 min), a recovery of 90%, and a purity of 100%.

3.2. Low-Abundance-Cell Selection via Physical Criteria

Differences in cell size, density, shape and deformability can be exploited in microsystems to select low-abundance cells on the basis of mechanical restriction (63, 64). Such microsystems are relatively easy to build with common microfabrication technologies (65).

The size and deformation characteristics of fetal nucleated red blood cells (fNRBCs) were used to isolate them from maternal blood (65). fNRBCs range between 9 and 12 μm in size and were demonstrated to deform and pass through fluidic obstacles fabricated in PDMS that were as small as 2.5 μm × 5 μm. WBCs ranging in diameter between 10 and 20 μm could not deform and thus were retained by the fluidic channels of similar dimensions. The authors (65) isolated low-abundance fNRBCs from umbilical blood that was preconcentrated using DGC. Unfortunately, the low processing rate of <0.35 ml h^{-1} posed a major challenge to this system, given that ~10 ml of blood had to be processed to accommodate sampling these low-abundance cells.

A series of massively parallel microfabricated sieving structures were used to separate neuroblastoma (NB) tumor cells from blood constituents on the basis of size characteristics (64). The reported devices consisted of four successively narrowing regions of channels. The size-based selection of tumor cells was carried out through the use of diluted blood (1:10) (v/v) containing the NB cells. As the NB cells traversed the device, they were retained in the 10-μm × 20-μm channels, but other blood cells migrated to the output. It was observed that in shallow channels NB cells tended to adhere to the walls upstream of where freely moving cells were retarded. A shorter (3.5-cm) device with deeper (20-μm) channels reduced the device flow resistance and adhesion problems. Experiments that used undiluted whole blood (2 ml) took approximately 3 h to analyze. The authors (64) noted that the enriched cells obtained from the device had low purity and that the interfering cells were composed of residual erythrocytes and leukocytes.

3.3. Low-Abundance-Cell Selection via Dielectrophoresis

DEP uses the electrical polarization of cells in nonuniform fields to induce translational motion and/or reorientation of the cells (66). The induced polarization depends on multiple factors related to the cells' condition, such as bilipid membrane characteristics, internal structure, and size of the nucleus (67). DEP has been used to study the physiology of bacterial (68), yeast (69), plant (70), and mammalian cells (71) and to investigate cellular alterations accompanying physiological changes, such as mitotic stimulation and induced differentiation. The variability in particular cells' response to electric fields can be used not only to differentiate cell types but also to distinguish the activation states of similar cells (72). DEP devices can differentiate among cell types by changing the field frequency or amplitude (73–75).

The DEP force (F_{DEP}) acting on a cell can be calculated via (76)

$$F_{DEP} = 2\pi\varepsilon_M r_p^3 R_e[f_{CM}(\omega)]\nabla E_{RMS}^2, \quad (6)$$

where ε_M is the permittivity of the suspending medium, r_P is the cell radius, E_{RMS} is the electric field strength, and $R_e[f_{CM}(\omega)]$ is the real part of the dipolar Clausius-Mossotti factor. This factor is the relative polarization of the cell versus that of the surrounding medium and is given by (76)

$$f_{CM}(\omega) = [\varepsilon_C^*(\omega) - \varepsilon_M^*(\omega)]/[\varepsilon_C^* + 2\varepsilon_M^*(\omega)], \quad (7)$$

where $\varepsilon_C{}^*$ and $\varepsilon_M{}^*$ are the complex permittivities of the cell and medium, respectively. The DEP forces can be either negative, $R_e[f_{CM}(\omega)] < 0$ (i.e., the cell is repelled by a region of higher electric field), or positive, $R_e[f_{CM}(\omega)] > 0$ (i.e., the cell is attracted to a region of higher electric field). As shown by Equations 6 and 7, the polarizability of the cell is frequency dependent; thus, changing ω can result in the selection of certain cell types.

A dielectric affinity column was used to select tumor cells (MDA231) from diluted blood (77), from which the cells were captured by balancing gravity, DEP, fluid drag, and hydrodynamic lift effects (**Figure 6**) and released by reducing the frequency of the applied electric field. Efficient

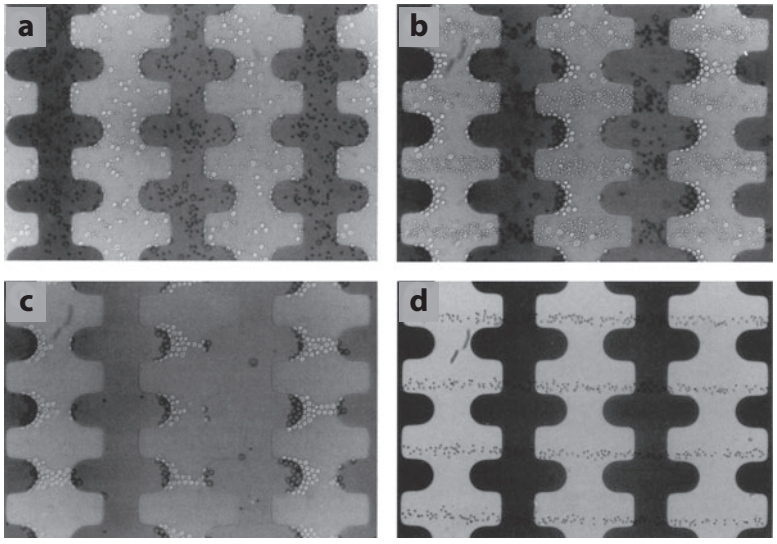

Figure 6

Dielectrophoretic separation of MDA231 human metastatic breast cancer cells from diluted peripheral blood. (*a*) Initial separation of cells in the chamber inlet well after the electrical sweep signal was applied. (*b*) Blood cells focused into bands that flowed between the electrode tips, leaving the cancer cells behind. (*c*) Cancer cells that remained on the electrode tips after the blood cells were swept downstream through the dielectrophoresis column. (*d*) Close to the chamber outlet well, where only blood cells in focused bands were moving. Reproduced with permission from Reference 77.

selection was obtained when (*a*) the product of the cell radii and dielectric polarizability was sufficiently different and (*b*) the ratio of fluid velocity to the square of the applied voltage was within the specified range, determined by the type of cell. The column sorted cells at a rate of $\sim$103 s^{-1}; larger devices increased this rate by two orders of magnitude. The viability of the excluded cells was 98%, indicating that the cell-membrane barrier function was maintained. The total number of cells analyzed with this device in a single run was 1.2×10^6, and the ratio of tumor cells to normal hematopoietic cells was 1:3.

The electrical conductivity of RBC membranes increases sharply when they become infected with malarial parasites such as *Plasmodium falciparum*. When challenged by a suspension in a low-conductivity medium, infected cells lose internal ions, whereas uninfected cells retain them (78). The resulting dielectric differences between infected and noninfected cells were exploited in order to sort these cells via DEP (78). Parasitized cells were isolated by steric dielectric field–flow fractionation (DEP-FFF) and were focused at the center of a spiral electrode array, identified, and counted. The spiral microelectrode array had a 2-mm^2 surface area and was composed of five complete turns of four parallel spiral elements. On the spiral array, cells were distinguished through differences in their DEP properties. More than 99.5% of the normal erythrocytes were trapped, and 90% of the parasitized cells were preconcentrated 50- to 200-fold.

Differences in cell-dielectric properties were exploited to separate and identify cells without extensive cell manipulation (79). For applications such as stem cell research, it is highly preferable that the isolated cells be unlabeled and minimally manipulated to preserve their integrity. Vykoukal and coworkers (80) applied DEP-FFF for the rapid, label-free enrichment of progenitor cells from a stromal vascular fraction. Different cell types were driven to different flow lamina in a DEP-FFF separator on the basis of the aggregate effect of their density and specific dielectric properties.

Low-abundance putative progenitor cells, NG2 cells (<2% in the starting mixture), were enriched up to 14-fold, yielding 28% $NG2^+$ cells in the most enriched fraction. This device is therefore ideally suited for batch-mode isolation and recovery of moderate quantities of cells ($<10^6$ cells per run).

μFACS: microfabricated fluorescence-activated cell sorting

Although these approaches are applicable to many cell-processing problems, they demand that the dielectric properties of the target cells be significantly different from those of the interfering cells. For this reason, DEP/gravitational field–flow fractionation (DEP/GFFF), which has a potentially higher discriminatory ability, has been developed (81, 82). GFFF is a process by which particles are allowed to settle while under the influence of an axial flow (83). In DEP/GFFF, the balance of DEP and gravitational forces controls cell position in the gravitational flow profile (82). This technique was applied to the separation of a breast cancer cell line (MDA435) from RBCs (83). Results suggested that the MDA435 cells could be separated from erythrocytes in a 10-μl sample containing a total of ~50,000 cells. The enriched fractions of the MDA435 cells and erythrocytes were reported to be >98% and >99%, respectively.

3.4. Low-Abundance-Cell Selection via Magnetic Interactions

Target cells can be specifically labeled with antibody-conjugated magnetic beads, and the selection and enrichment of the low-abundance cells can be achieved through the use of a magnetic field. Using this principle, Lee and coworkers (84) developed an integrated system capable of selecting RNA viruses, such as dengue virus and enterovirus, through use of antibody-conjugated magnetic beads and one-step RT-PCR in an integrated microfluidic system. The target virus in the sample was captured with modified magnetic beads and manipulated via microelectromagnets (**Figure 7*a***). The integrated microfluidic system performed the entire process automatically with a rotary micropump and microvalves for fluid control. Following isolation, the viruses selected were subjected to thermolysis, RNA extraction, and RT-PCR on a single chip. The authors' results were similar to those obtained with benchtop instruments (**Figure 7*b***).

Beyor and coworkers (85) presented an *E. coli* O157:H7-detection microsystem with integrated cell capture, sample preparation, and PCR with capillary electrophoresis analysis. Immunomagnetic beads were coupled to polyclonal antibodies specific to the *E. coli* phenotype of interest. Sample volumes ranging from 10 to 100 μl were introduced and driven through immunomagnetic bead beds to capture the target cells. A detection limit of 0.2 colony-forming units μl^{-1} was achieved for an input volume of 50 μl.

3.5. Microfluidic Fluorescence-Activated Cell Sorting

Replacing the conventional flow chamber in FACS with microfabricated devices could allow more sensitive optical detection, easier mechanical setup, and more innovative sorting schemes. Another advantage is that multiple cell sorters can be fabricated in parallel on a single chip, allowing increased throughput or successive enrichment steps. Fu et al. (86) demonstrated a complete microfabricated fluorescence-activated cell sorting (μFACS) device for *E. coli* HB101 cells. The chip was mounted on an inverted optical microscope, and fluorescence readout with a photomultiplier tube was accomplished at a T-shaped fluidic junction on the chip, with the cells manipulated electrokinetically. An advantage of the μFACS system is the small detection volume, typically 250 fl, which greatly reduces background fluorescence from the cell suspension and chamber material. Low-abundance cells are sorted by implementing a specific sorting algorithm. When a cell of interest is detected, the flow is stopped and the cell of interest is recovered by running the flow backward at a slow speed until the cell is moved into a collection channel. At that point, the cell is

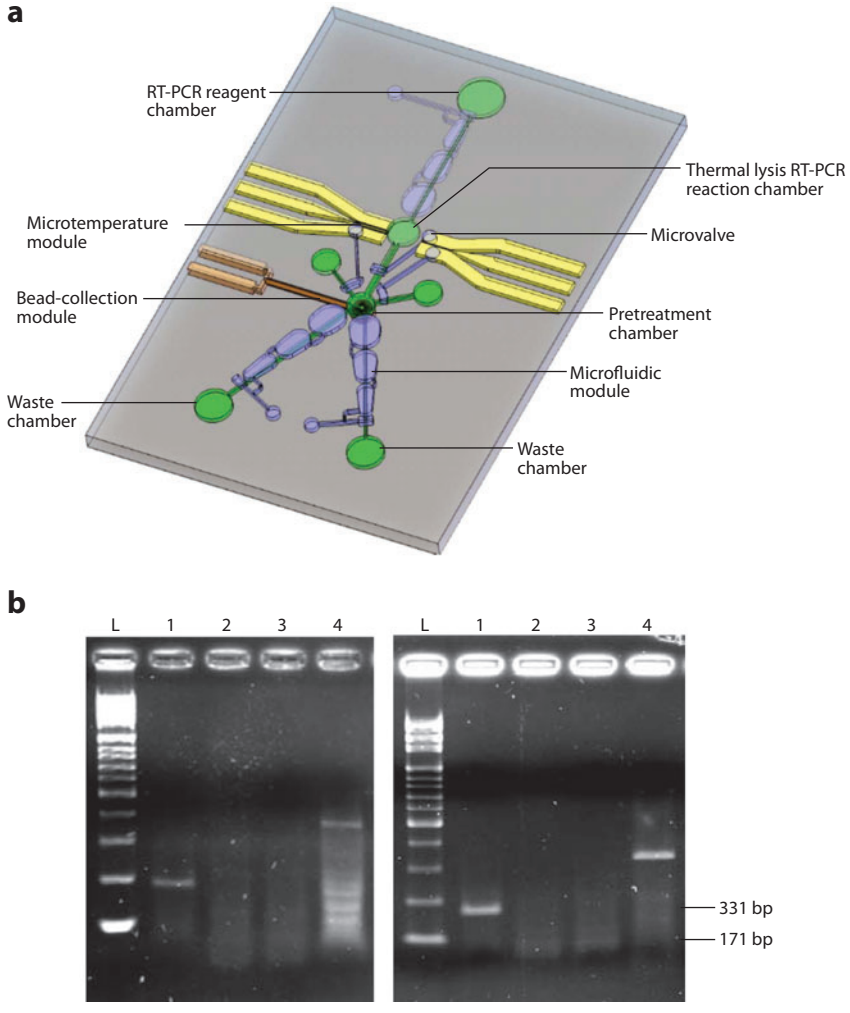

Figure 7

(*a*) Schematic of an integrated reverse-transcription polymerase chain reaction (RT-PCR) chip with a cell-selection unit for the magnetic capture of target cells. A microtemperature module, a bead-collection module, and a microfluidic control module are integrated into the chip. (*b*) A mixture of dengue virus (10^2 PFU) and enterovirus 71 (10^2 PFU) was incubated with antidengue antibody (lanes 1 and 2) or antienterovirus 71 antibody-conjugated magnetic beads (lanes 3 and 4); RT-PCR was then performed with dengue group–specific primers (lanes 1 and 3) or enterovirus 71–specific primers (lanes 2 and 4). The lanes marked with the letter L represent signals generated from DNA size markers. Results on the left and right are from a benchtop instrument and the integrated chip, respectively. Reproduced with permission from Reference 84.

collected, and the device is once again run at a high speed in the forward direction. This reversible sorting method cannot be performed with standard FACS machines. The μFACS system offers several advantages over traditional FACS: (*a*) Because the channels are made with micrometer-size dimensions, the volume of the interaction region can be precisely controlled, eliminating the need for hydrodynamic focusing; (*b*) the planar geometry of the device allows for the use of

high–numerical aperture optics, increasing the limit of detection of the optical system; and (*c*) the disposability of the sorting device obviates the need for cleaning and sterilizing the instrument and prevents cross contamination between samples. However, the throughput obtained with this μFACS is 20 cells s^{-1}, considerably lower than that of conventional FACS.

Another example of low-abundance-cell sorting via μFACS was presented by Simonnet & Groisman (87), who attempted to port conventional high-throughput, high-resolution cell sorting using flow cytometry to a PDMS microsystem. The integrated cell sorter was incorporated with various components, including peristaltic pumps, dampers, and input and output wells, to perform cell sorting in a coordinated and automated fashion. DEP and pressure switching were used to create a valveless device for the separation of cells within microchannels. The standard forward and reverse sorting algorithms were implemented. Conventional FACS uses flow rates of ~10 m s^{-1}, corresponding to sampling rates of 1,000–50,000 cells s^{-1}. Using this platform, the authors processed up to 17,000 cells s^{-1}. An 83-fold enrichment was achieved in a single pass, yielding 40% recovery. As with the macroscale version of FACS, sorting and enumerating low-abundance cells require specific staining protocols as well as sample-preprocessing steps.

SUMMARY POINTS

1. The selection and enumeration of low-abundance cells from complex and heterogeneous samples have many important applications in clinical, environmental, and national security areas.
2. Four important metrics concerning the performance of low-abundance cell technologies must be evaluated: (*a*) throughput, (*b*) recovery, (*c*) purity, and (*d*) viability.
3. Although the microscale performance metrics of recovery, purity, and viability are comparable to their macroscale counterparts, the throughput of microsystems is typically inferior.
4. Commercially available macroscale systems allow the collection of low-abundance cells, but their implementation is fraught with challenges, such as labor-intensive sample handling, sample loss due to transfer from instrument to instrument, and the use of fluorescence microscopy for cell enumeration.
5. Microfluidic-based systems can provide processing strategies that are difficult to implement in macroscale platforms and that generate environments that are more conducive to maintaining the viability of rare cells, making them available for culturing and subsequent molecular analysis.
6. IMACS, FACS, and size-based selection techniques of low-abundance cells can be transitioned to microscale systems, and they can produce results that are similar if not superior to their macroscale counterparts. Moreover, the high automation potential of microfluidic systems and their ability to process samples in closed architectures provide a venue in which to analyze mass-limited samples, such as low-abundance cells, that is free from contamination.
7. Unique processing strategies for selecting low-abundance cells can be employed in microsystems such as DEP and DEP-hybrid-based techniques.

FUTURE ISSUES

1. The selection and enumeration of low-abundance cells are often not the terminal steps in the processing pipeline of these cells. For example, CTCs selected via immunoaffinity, with EpCAM as the molecular target, can originate from a variety of different cancers, such as colorectal, prostate, bladder, lung, or breast. To determine the specific type of cancer, it is necessary to molecularly profile the selected cells.
2. For mass-limited samples, it is necessary to integrate molecular processing tasks with the cell-selection device to produce functional systems that do not require samples to be transferred from instrument to instrument, which can result in sample loss and/or contamination.
3. Highly integrated low-abundance cell–based microfluidic devices that can molecularly profile such cells will find applications in medicine at the point of care; national security and counterterrorism; police, paramedics, and fire departments; veterinary medicine; and environmental and food safety monitoring.
4. A major challenge concerns the mass-limited samples encountered when analyzing low-abundance cells. For example, in a single eukaryotic cell two copies of the genome and approximately 300 copies of each different mRNA molecule are present, requiring highly sensitive genotyping techniques to characterize these molecular entities.
5. For immunoaffinity-based positive selection of rare cells, the recovery should be made independent of the expression level of the integral membrane protein used as the antigenic target.
6. Microsystems for rare cell selection need to be designed to sample larger input volumes in reasonable times (i.e., higher throughput) to accommodate extremely low abundance cells.

DISCLOSURE STATEMENT

The authors are not aware of any affiliations, memberships, funding, or financial holdings that might be perceived as affecting the objectivity of this review.

ACKNOWLEDGMENTS

The authors would like to thank the National Institutes of Health (National Cancer Institute, R33 CA099246-01) for partial financial support of their work. Their work was also supported in part by the National Science Foundation, under grant number EPS-0346411, and the State of Louisiana Board of Regents Support Fund.

LITERATURE CITED

1. Berger MJ, Adams SD, Tigges BM, Sprague SL, Wang XJ, et al. 2006. Differentiation of umbilical cord blood–derived multilineage progenitor cells into respiratory epithelial cells. *Cytotherapy* 8:480–87
2. Mostert B, Sleijfer S, Foekens JA, Gratama JW. 2009. Circulating tumor cells (CTCs): detection methods and their clinical relevance in breast cancer. *Cancer Treat. Rev.* 35:463–74

3. Utikal J, Polo JM, Stadtfeld M, Maherali N, Kulalert W, et al. 2009. Immortalization eliminates a roadblock during cellular reprogramming into iPS cells. *Nature* 460:1145–48
4. Elisavet K, Aggelki K, Nikolas P, Aris A. 2009. Evaluation of non-invasive prenatal diagnosis from fetal nucleated red blood cells (NRBCs) isolated from maternal circulation. *Chromosome Res.* 17(Suppl. 1):230–31
5. de Wynter E, Ploemacher RE. 2001. Assays for the assessment of human hematopoietic stem cells. *J. Biol. Regul. Homeost. Agents* 15:23–27
6. Allard WJ, Matera J, Miller MC, Repollet M, Connelly MC, et al. 2004. Tumor cells circulate in the peripheral blood of all major carcinomas but not in healthy subjects or patients with nonmalignant diseases. *Clin. Cancer Res.* 10:6897–904
7. Bertazza L, Mocellin S, Nitti D. 2008. Circulating tumor cells in solid cancer: tumor marker of clinical relevance? *Curr. Oncol. Rep.* 10:137–46
8. Mocellin S, Hoon D, Ambrosi A, Nitti D, Rossi CR. 2006. The prognostic value of circulating tumor cells in patients with melanoma: a systematic review and meta-analysis. *Clin. Cancer Res.* 12:4605–13
9. Nagrath S, Sequist LV, Maheswaran S, Bell DW, Irimia D, et al. 2007. Isolation of rare circulating tumor cells in cancer patients by microchip technology. *Nature* 450:1235–39
10. Siewert C, Herber M, Hunzelmann N, Fodstad O, Miltenyi S, et al. 2001. Rapid enrichment and detection of melanoma cells from peripheral blood mononuclear cells by a new assay combining immunomagnetic cell sorting and immunocytochemical staining. *Recent Results Cancer Res.* 158:51–60
11. Wuelfing P, Borchard J, Buerger H, Heidl S, Zaenker KS, et al. 2006. HER2-positive circulating tumor cells indicate poor clinical outcome in stage I to III breast cancer patients. *Clin. Cancer Res.* 12:1715–20
12. Jansen CA, De Cuyper IM, Hooibrink B, Van Der Bij AK, van Baarle D, Miedema F. 2006. Prognostic value of HIV-1 gag-specific $CD4^+$ T-cell responses for progression to AIDS analyzed in a prospective cohort study. *Blood* 107:1427–33
13. Ramirez de Arellano E, Martin C, Soriano V, Alcami J, Holguin A. 2007. Genetic analysis of the long terminal repeat (LTR) promoter region in HIV-1-infected individuals with different rates of disease progression. *Virus Genes* 34:111–16
14. Collins DP, Luebering BJ, Shaut DM. 1998. T-lymphocyte functionality assessed by analysis of cytokine receptor expression, intracellular cytokine expression, and femtomolar detection of cytokine secretion by quantitative flow cytometry. *Cytometry* 33:249–55
15. Deng MQ, Cliver DO, Mariam TW. 1997. Immunomagnetic capture PCR to detect viable *Cryptosporidium parvum* oocysts from environmental samples. *Appl. Environ. Microbiol.* 63:3134–38
16. Islam D, Lindberg AA. 1992. Detection of *Shigella dysenteriae* type 1 and *Shigella flexneri* in feces by immunomagnetic isolation and polymerase chain reaction. *J. Clin. Microbiol.* 30:2801–6
17. Seesod N, Nopparat P, Hedrum A, Holder A, Thaithong S, et al. 1997. An integrated system using immunomagnetic separation, polymerase chain reaction, and colorimetric detection for diagnosis of *Plasmodium falciparum*. *Am. J. Trop. Med. Hyg.* 56:322–28
18. El-Ali J, Sorger PK, Jensen KF. 2006. Cells on chips. *Nature* 442:403–11
19. Kodituwakku AP, Jessup C, Zola H, Roberton DM. 2003. Isolation of antigen-specific B cells. *Immunol. Cell Biol.* 81:163–70
20. Adams AA, Okagbare PI, Feng J, Hupert ML, Patterson D, et al. 2008. Highly efficient circulating tumor cell isolation from whole blood and label-free enumeration using polymer-based microfluidics with an integrated conductivity sensor. *J. Am. Chem. Soc.* 130:8633–41
21. Adams AA. 2008. *Novel Devices and Protocols Enabling Isolation and Enumeration of Low Abundant Biological Cells from Complex Matrices*. Baton Rouge: La. State Univ. 190 pp.
22. Mohamed H, Murray M, Turner JN, Caggana M. 2005. Circulating tumor cells: capture with a micromachined device. *Proc. NSTI Nanotechnol. Conf. Trade Show* 1:1–4
23. Furdui VI, Harrison DJ. 2001. Immunomagnetic separation of rare cells on chip for DNA assay sample preparation. *Proc. Micro Total Anal. Syst. Symp., 5th, Monterey*, pp. 289–90. Enschede, Neth.: Kluwer Acad.
24. Grodzinski P, Yang J, Liu RH, Ward MD. 2003. A modular microfluidic system for cell pre-concentration and genetic sample preparation. *Biomed. Microdevices* 5:303–10

25. Vona G, Sabile A, Louha M, Sitruk V, Romana S, et al. 2000. Isolation by size of epithelial tumor cells: a new method for the immunomorphological and molecular characterization of circulating tumor cells. *Am. J. Pathol.* 156:57–63
26. Wilding P, Pfahler J, Bau HH, Zemel JN, Kricka LJ. 1994. Manipulation and flow of biological fluids in straight channels micromachined in silicon. *Clin. Chem.* 40:43–47
27. Balic M, Dandachi N, Lin H, Datar RH. 2005. Cancer metastasis: Advances in the detection and characterization of disseminated tumor cells facilitate clinical translation. *Natl. Med. J. India* 18:250–55
28. Ghossein RA, Osman I, Bhattacharya S, Ferrara J, Fazzari M, et al. 1999. Detection of prostatic specific membrane antigen messenger RNA using immunobead reverse transcriptase polymerase chain reaction. *Diagn. Mol. Pathol.* 8:59–65
29. Hayes DF, Smerage J. 2008. Is there a role for circulating tumor cells in the management of breast cancer? *Clin. Cancer Res.* 14:3646–50
30. Balic M, Dandachi N, Hofmann G, Samonigg H, Loibner H, et al. 2005. Comparison of two methods for enumerating circulating tumor cells in carcinoma patients. *Cytom. B Clin. Cytom.* 68:25–30
31. Said TM, Agarwal A, Zborowski M, Grunewald S, Glander H-J, Paasch U. 2008. Utility of magnetic cell separation as a molecular sperm preparation technique. *J. Androl.* 29:134–42
32. Zabaglo L, Ormerod MG, Dowsett M. 2000. Measurement of markers for breast cancer in a model system using laser scanning cytometry. *Cytometry* 41:166–71
33. Gross HJ, Verwer B, Houck D, Hoffman RA, Recktenwald D. 1995. Model study detecting breast cancer cells in peripheral blood mononuclear cells at frequencies as low as 10^{-7}. *Proc. Natl. Acad. Sci. USA* 92:537–41
34. Bosma AJ, Weigelt B, Lambrechts AC, Verhagen OJHM, Pruntel R, et al. 2002. Detection of circulating breast tumor cells by differential expression of marker genes. *Clin. Cancer Res.* 8:1871–77
35. Helo P, Cronin AM, Danila DC, Wenske S, Gonzalez-Espinoza R, et al. 2009. Circulating prostate tumor cells detected by reverse transcription–PCR in men with localized or castration-refractory prostate cancer: concordance with CellSearch assay and association with bone metastases and with survival. *Clin. Chem.* 55:765–73
36. Belov L, Huang P, Chrisp JS, Mulligan SP, Christopherson RI. 2005. Screening microarrays of novel monoclonal antibodies for binding to T-, B- and myeloid leukaemia cells. *J. Immunol. Methods* 305:10–19
37. Pappas D, Wang K. 2007. Cellular separations: a review of new challenges in analytical chemistry. *Anal. Chim. Acta* 601:26–35
38. Sitar G, Brambati B, Baldi M, Montanari L, Vincitorio M, et al. 2004. The use of nonphysiological conditions to isolate fetal cells from maternal blood. *Exp. Cell Res.* 302:153–61
39. Russell TR, McGann P, Music M, Ciocci M. 2004. Methods and reagents for improved selection of biological materials. *US Patent Appl. No. 2002–208939 2004023222*
40. Chen Z, Zhang S, Tang Z, Xiao P, Guo X, Lu Z. 2006. Pool-dam structure based microfluidic devices for filtering tumor cells from blood mixtures. *Surf. Interface Anal.* 38:996–1003
41. Lord BI. 1997. Stem. cell chemokine for hematopoietic recovery. *WO Patent Appl. No. 96–GB2006 9706817*
42. Hamada S, Hara K, Hamada T, Yasuda H, Moriyama H, et al. 2009. Upregulation of the mammalian target of rapamycin complex 1 pathway by Ras homolog enriched in brain in pancreatic β-cells leads to increased β-cell mass and prevention of hyperglycemia. *Diabetes* 58:1321–32
43. Graham HA, Gorman JG, Rowell JP. 2007. Magnetic particle tagged blood bank reagents and techniques. *US Patent Appl. No. 2007–715411 2007172899*
44. Pan WJ, Haut PR, Olszewski M, Kletzel M. 1999. Two-day collection and pooling of peripheral blood stem cells with semiautomated density gradient cell separation. *J. Hematother. Stem Cell Res.* 8:561–64
45. Iacone A, Quaglietta AM, D'Antonio D, Accorsi P, Dragani A, et al. 1991. Density gradient separation of hematopoietic stem cells in autologous bone marrow transplantation. *Haematologica* 76(Suppl. 1):18–21
46. Wagner JE Jr. 1993. Umbilical cord blood stem cell transplantation: current status and future prospects (1992). *J. Hematother.* 2:225–28

47. Beebe DJ, Moore JS, Yu Q, Liu RH, Kraft ML, et al. 2000. Microfluidic tectonics: a comprehensive construction platform for microfluidic systems. *Proc. Natl. Acad. Sci. USA* 97:13488–93
48. Lagally ET, Simpson PC, Mathies RA. 2000. Monolithic integrated microfluidic DNA amplification and capillary electrophoresis analysis system. *Sens. Actuators B* 63:138–46
49. Mairhofer J, Roppert K, Ertl P. 2009. Microfluidic systems for pathogen sensing: a review. *Sensors* 9:4804–23
50. Koo OK, Liu YS, Shuaib S, Bhattacharya S, Ladisch MR, et al. 2009. Targeted capture of pathogenic bacteria using a mammalian cell receptor coupled with dielectrophoresis on a biochip. *Anal. Chem.* 81:3094–101
51. Chang KC, Hammer DA. 1999. The forward rate of binding of surface-tethered reactants: effect of relative motion between two surfaces. *Biophys. J.* 76:1280–92
52. Katkov II, Mazur P. 1999. Factors affecting yield and survival of cells when suspensions are subjected to centrifugation influence of centrifugal acceleration, time of centrifugation, and length of the suspension column in quasi-homogeneous centrifugal fields. *Cell Biochem. Biophys.* 31:231–45
53. Maheswaran S, Sequist LV, Nagrath S, Ulkus L, Brannigan B, et al. 2008. Detection of mutations in EGFR in circulating lung-cancer cells. *N. Engl. J. Med.* 359:366–77
54. Heinze BC, Song J-Y, Lee C-H, Najam A, Yoon J-Y. 2009. Microfluidic immunosensor for rapid and sensitive detection of bovine viral diarrhea virus. *Sens. Actuators B* 138:491–96
55. Lin P, Ghetti A, Shi W, Tang M, Harvie GI, et al. 2008. Methods and compositions for detecting rare cells from a biological sample esp. tumor cells from body fluids. *US Patent Appl. No. 2007–777962 2008057505*
56. Sardana G, Jung K, Stephan C, Diamandis EP. 2008. Proteomic analysis of conditioned media from the PC3, LNCaP, and 22Rv1 prostate cancer cell lines: discovery and validation of candidate prostate cancer biomarkers. *J. Proteome Res.* 7:3329–38
57. Steeg PS. 2006. Tumor metastasis: mechanistic insights and clinical challenges. *Nature* 12:895–904
58. Diener JL, Hatala P, Killough JR, Wagner-Whyte J, Wilson C, Zhu S. 2006. Stabilized aptamers to PSMA and their use in diagnosis and treatment of prostate cancer. *WO Patent Appl. No. 2006–US8193 2006096754*
59. Tombelli S, Minunni M, Mascini M. 2007. Aptamer-based assays for diagnostics, environmental and food analysis. *Biomol. Eng.* 24:191–200
60. Shangguan D, Tang Z, Mallikaratchy P, Xiao Z, Tan W. 2007. Optimization and modifications of aptamers selected from live cancer cell lines. *ChemBioChem* 8:603–6
61. Dharmasiri U, Balamurugan S, Adams AA, Okagbare PI, Obubuafo A, Soper SA. 2009. Highly efficient capture and enumeration of low abundance prostate cancer cells using prostate-specific membrane antigen aptamers immobilized to a polymeric microfluidic device. *Electrophoresis* 30:1–12
62. Hakomori S. 1990. Bifunctional role of glycosphingolipids. Modulators for transmembrane signaling and mediators for cellular interactions. *J. Biol. Chem.* 265:18713–16
63. Harrison DJ, Manz A, Fan Z, Luedi H, Widmer HM. 1992. Capillary electrophoresis and sample injection systems integrated on a planar glass chip. *Anal. Chem.* 64:1926–32
64. Mohamed H, McCurdy LD, Szarowski DH, Duva S, Turner JN, Caggana M. 2004. Development of a rare cell fractionation device: application for cancer detection. *IEEE Trans. Nanobiosci.* 3:251–56
65. Mohamed H, Turner JN, Caggana M. 2007. Biochip for separating fetal cells from maternal circulation. *J. Chromatogr. A* 1162:187–92
66. Baek SH, Chang W-J, Baek J-Y, Yoon DS, Bashir R, Lee SW. 2009. Dielectrophoretic technique for measurement of chemical and biological interactions. *Anal. Chem.* 81:7737–42
67. Hakota M, Hibino H, Fukuda H, Shiba Y. 2009. Cell separators. *Jpn. Patent Appl. No. 2007–247809 2009077638*
68. Yoo J, Cha M, Lee J. 2008. Bacterial concentration detection with dielectrophoresis and capacitive measurement. *Proc. NSTI Nanotechnol. Conf. Trade Show* 2:611–14
69. Huang J-T, Wang G-C, Tseng K-M, Fang S-B. 2008. A chip for catching, separating, and transporting bio-particles with dielectrophoresis. *J. Ind. Microbiol. Biotechnol.* 35:1551–57
70. Saito M, Horikiri S, Matsuoka H. 2003. Dielectrophoretic selection of viable single-cells of rice and tobacco. *Electrochemistry* 71:446–48
71. Gascoyne PRC, Noshari J, Anderson TJ, Becker FF. 2009. Isolation of rare cells from cell mixtures by dielectrophoresis. *Electrophoresis* 30:1388–98

72. An J, Lee J, Lee SH, Park J, Kim B. 2009. Separation of malignant human breast cancer epithelial cells from healthy epithelial cells using an advanced dielectrophoresis-activated cell sorter (DACS). *Anal. Bioanal. Chem.* 394:801–9
73. Hu Q, Joshi RP, Beskok A. 2009. Model study of electroporation effects on the dielectrophoretic response of spheroidal cells. *J. Appl. Phys.* 106:024701
74. Jang L-S, Huang P-H, Lan K-C. 2009. Single-cell trapping utilizing negative dielectrophoretic quadrupole and microwell electrodes. *Biosens. Bioelectron.* 24:3637–44
75. Wang M-W. 2009. Using dielectrophoresis to trap nanobead/stem cell compounds in continuous flow. *J. Electrochem. Soc.* 156:G97–102
76. Gascoyne PRC, Vykoukal J. 2002. Particle separation by dielectrophoresis. *Electrophoresis* 23:1973–83
77. Becker FF, Wang X-B, Huang Y, Pethig R, Vykoukal J, Gascoyne PRC. 1995. Separation of human breast cancer cells from blood by differential dielectric affinity. *Proc. Natl. Acad. Sci. USA* 92:860–64
78. Gascoyne P, Mahidol C, Ruchirawat M, Satayavivad J, Watcharasit P, Becker FF. 2002. Microsample preparation by dielectrophoresis: isolation of malaria. *Lab Chip* 2:70–75
79. Labeed FH, Coley HM, Hughes MP. 2006. Differences in the biophysical properties of membrane and cytoplasm of apoptotic cells revealed using dielectrophoresis. *Biochim. Biophys. Acta Gen. Subj.* 1760:922–29
80. Vykoukal J, Vykoukal DM, Freyberg S, Alt EU, Gascoyne PRC. 2008. Enrichment of putative stem cells from adipose tissue using dielectrophoretic field–flow fractionation. *Lab Chip* 8:1386–93
81. Huang Y, Wang X-B, Becker FF, Gascoyne PRC. 1996. Membrane changes associated with the temperature-sensitive $P85^{gag-mos}$-dependent transformation of rat kidney cells as determined by dielectrophoresis and electrorotation. *Biochim. Biophys. Acta Biomembr.* 1282:76–84
82. Markx GH, Rousselet J, Pethig R. 1997. DEP-FFF: field-flow fractionation using nonuniform electric fields. *J. Liq. Chromatogr. Relat. Technol.* 20:2857–72
83. Yang J, Huang Y, Wang X-B, Becker FF, Gascoyne PRC. 1999. Cell separation on microfabricated electrodes using dielectrophoretic/gravitational field–flow fractionation. *Anal. Chem.* 71:911–18
84. Lee W-C, Lien K-Y, Lee G-B, Lei H-Y. 2008. An integrated microfluidic system using magnetic beads for virus detection. *Diagn. Microbiol. Infect. Dis.* 60:51–58
85. Beyor N, Seo TS, Liu P, Mathies RA. 2008. Immunomagnetic bead–based cell concentration microdevice for dilute pathogen detection. *Biomed. Microdevices* 10:909–17
86. Fu AY, Chou H-P, Spence C, Arnold FH, Quake SR. 2002. An integrated microfabricated cell sorter. *Anal. Chem.* 74:2451–57
87. Simonnet C, Groisman A. 2006. High-throughput and high-resolution flow cytometry in molded microfluidic devices. *Anal. Chem.* 78:5653–63
88. Sumi S, Arai K, Kitahara S, Yoshida KI. 2000. Preliminary report of the clinical performance of a new urinary bladder cancer antigen test: comparison to voided urine cytology in the detection of transitional cell carcinoma of the bladder. *Clin. Chim. Acta* 296:111–20
89. Liang X, Xu K, Xu J, Chen W, Shen H, Liu J. 2009. Preparation of immunomagnetic nanoparticles and their application in the separation of mouse $CD34^+$ hematopoietic stem cells. *J. Magn. Magn. Mater.* 321:1885–88
90. Gangopadhyay NN, Shen H, Landreneau R, Luketich JD, Schuchert MJ. 2004. Isolation and tracking of a rare lymphoid progenitor cell which facilitates bone marrow transplantation in mice. *J. Immunol. Methods* 292:73–81
91. Muscari C, Gamberini C, Carboni M, Basile I, Farruggia G, et al. 2007. Different expression of NOS isoforms in early endothelial progenitor cells derived from peripheral and cord blood. *J. Cell. Biochem.* 102:992–1001
92. Horsman KM, Barker SLR, Ferrance JP, Forrest KA, Koen KA, Landers JP. 2005. Separation of sperm and epithelial cells in a microfabricated device: potential application to forensic analysis of sexual assault evidence. *Anal. Chem.* 77:742–49
93. Terry VH, Johnston ICD, Spina CA. 2009. CD44 microbeads accelerate HIV-1 infection in T cells. *Virology* 388:294–304
94. Wagner C, Kotsougiani D, Pioch M, Prior B, Wentzensen A, Haensch GM. 2008. T lymphocytes in acute bacterial infection: increased prevalence of $CD11b^+$ cells in the peripheral blood and recruitment to the infected site. *Immunology* 125:503–09

95. Yang S-Y, Lien K-Y, Huang K-J, Lei H-Y, Lee G-B. 2008. Micro flow cytometry utilizing a magnetic bead–based immunoassay for rapid virus detection. *Biosens. Bioelectron.* 24:855–62
96. Kubota-Koketsu R, Mizuta H, Oshita M, Ideno S, Yunoki M, et al. 2009. Broad neutralizing human monoclonal antibodies against influenza virus from vaccinated healthy donors. *Biochem. Biophys. Res. Commun.* 387:180–85

Annual Review of
Analytical Chemistry

Volume 3, 2010

Contents

Indexes

Errata

An online log of corrections to *Annual Review of Analytical Chemistry* articles may be found at http://arjournals.annualreviews.org/errata/anchem.